Title: CoZnAl catalysts for ethanol steam reforming reaction

Authors: M. Noelia Barroso, Manuel F. Gomez, Luis A. Arrúa, M. Cristina Abello

PII: S1385-8947(09)00757-8
DOI: doi:10.1016/j.cej.2009.10.064
Reference: CEJ 6628

To appear in: *Chemical Engineering Journal*

Received date: 16-6-2009
Revised date: 28-10-2009
Accepted date: 30-10-2009

Please cite this article as: M.N. Barroso, M.F. Gomez, L.A. Arrúa, M.C. Abello, CoZnAl catalysts for ethanol steam reforming reaction, *Chemical Engineering Journal* (2008), doi:10.1016/j.cej.2009.10.064

CoZnAl CATALYSTS FOR ETHANOL STEAM REFORMING REACTION

M. Noelia Barroso, Manuel F. Gomez, Luis A. Arrúa, M. Cristina Abello*

Instituto de Investigaciones en Tecnología Química - (UNSL-CONICET). Chacabuco y Pedernera, (5700) San Luis, Argentina. E-mail: cabello@unsl.edu.ar

Abstract

The ethanol steam reforming was studied at 500 and 600 °C on CoZnAl catalysts with different Co loading (9 and 25 wt.%) and a Zn:Al atomic ratio nearly constant (Zn:Al ≅ 0.6). The catalysts were prepared by the citrate sol gel method and characterized by different techniques such as AA, TG, BET, TPR, XRD, RAMAN and SEM-EDX. They were active in the ethanol steam reforming at atmospheric pressure in the temperature range studied, but with significant differences in their performance. High hydrogen selectivities, better than 80%, were obtained on catalyst with high Co loading (25 wt.%). CO, CO_2 and minor amount of CH_4 were the only carbon products at 600 °C.

Keywords. Ethanol steam reforming, hydrogen production, CoZnAl catalysts

1. Introduction

The recent world-wide interest in the energy area is strongly focused on the development of alternative fuels. In this context, the hydrogen fuel cells are the most promising systems and the key is an efficient hydrogen production. Among several possibilities, the production of hydrogen from steam reforming of ethanol (SRE) is gaining great attention and may become an important industrial process [1, 2]. Ethanol has several advantages compared to other raw materials but the most important are its renewable origin and the consequent reduction in CO_2 emission. Ethanol can be obtained from biomass fermentation (e.g.: corn, sugar cane, cellulose, etc.). It slightly contributes to green house effect since CO_2 is recycled through photosynthesis during the plant growth. Moreover, it has a relatively high hydrogen content and its reaction with water under steam-reforming conditions is able to produce 6 mol of H_2 per mole of reacted ethanol:

$$CH_3CH_2OH + 3H_2O \rightarrow 6H_2 + 2CO_2$$

Different catalysts have been studied for this reaction including oxides [1], nickel- [3-5], nickel–copper- [6, 7] and noble metals- [8–11]. Cobalt-based catalysts have also been investigated but they have received much less attention [12–20]. Haga et al. [12] studied the steam reforming of ethanol over cobalt supported on Al_2O_3, SiO_2, ZrO_2, MgO and activated carbon. The catalysts with 7.4 Co wt% prepared by impregnation method were tested under diluted conditions. Co/Al_2O_3 showed the best performance at 400 °C and a water: ethanol molar ratio of 4.2. The authors suggested that the support properties were the decisive factors regarding the selectivity for steam reforming although deactivation studies were not reported. Batista et al. [16] have also carried out a comparative study over Co/Al_2O_3, Co/MgO and Co/SiO_2 catalysts prepared by dry impregnation method. High conversion level (> 90%) were obtained but a considerable carbon amount after 9 h in reaction was deposited in all catalysts, the largest being for Co/Al_2O_3 (24.6 wt%). The authors assumed that the alumina acid sites were responsible to promote the ethanol cracking and dehydration to ethylene. A kinetic study over Co(15 wt%)/Al_2O_3 has been reported [17] from which the optimum operating conditions in order to achieve H_2 rich product stream with minimum CO and CH_4 were 500 °C, molar ratio = 3-5 and contact time (W/F) 15 -17 kg_{cat}/(mol/s). The kinetic model reasonably fit the experimental data collected between 3 and 7 h in time on stream but it can not predict the complete catalyst behavior because the observed deactivation process was not taken into account. Llorca et al. [15] studied Co catalysts supported on ZnO which were very effective in the SRE reaction, but showed an abundant carbon deposition. The interactions of Co species on ZrO_2 and TiO_2 have been studied [18] and metallic cobalt sites were found to correlate with the SRE activity. Recently, the effect of cerium oxide on Co-based catalyst stability has also been reported [19, 20]

In this work, unsupported CoZnAl catalysts are examined in ethanol steam reforming and the influence of Co loading is discussed. The citrate method is used for catalyst preparation. Characterization studies that included AA, BET, TPR, XRD, TG-TPO, Raman and SEM-EDX are presented as well.

2. Experimental

2.1. Catalyst preparation

CoZnAl catalysts were prepared by the citrate method. Citric acid was added to an aqueous solution that contained all the required ions as metal nitrates ($Co(NO_3)_2$. $6H_2O$; $Zn(NO_3)_2.6H_2O$; $Al(NO_3)_3.9H_2O$). An equivalent of acid per total equivalent of metals was used. The solution was stirred for 10 min and held at boiling temperature for 30 min. Then the solution was concentrated by evaporation under vacuum in a Rotavapor at 75 °C until a viscous liquid was obtained. Finally dehydration was completed by drying the sample in a vacuum oven at 100 °C for 16 h. The samples were calcined under the following program: at 450 °C in N_2 flow for 2 h, a heating from 450 to 500 °C in O_2 (10%)/N_2 flow, then at 500 °C for 5 h and finally the temperature was raised to 700 °C for 2 h. The samples were denoted as CoZAx where "x" indicates the cobalt weight %.

2.2. Catalyst characterization

All samples were characterized using different physico - chemical methods.

Chemical composition. Chemical composition was determined by atomic absorption spectroscopy. Alkali fusion with $KHSO_4$ and a subsequent dissolution with diluted HCl brought the samples into solution. The measurements were carried out using a Varian AA50 equipment.

BET Surface area. BET surface areas were measured by using a Micromeritics Accusorb 2100E instrument by adsorption of nitrogen at –196 °C on 200 mg of sample previously degassed at 200 °C for 2 h under a high vacuum atmosphere.

X-ray Diffraction (XRD). XR diffraction patterns were obtained with a RIGAKU diffractometer operated at 30 kV and 20 mA by using Ni-filtered CuKα radiation (λ= 0.15418 nm) at a rate of 3° min^{-1} from 2θ = 20° to 90°. The powdered samples were analyzed without a previous treatment after deposition on a quartz sample holder. The identification of crystalline phases was made by matching with the JCPDS files.

Thermal gravimetry (TG). The analyses were recorded by using TGA 51 Shimadzu equipment. The samples, i.a. 15 mg, were placed in a Pt cell and heated from room temperature to 1000 °C at a heating rate of 10 °C min^{-1} with a gas feed (air or N_2) of 50 mL min^{-1}.

Temperature programmed reduction (TPR). Studies were performed in a conventional TPR equipment. This apparatus consists of a gas handling system with mass flow controllers (Matheson), a tubular reactor, a linear temperature programmer (Omega, model CN 2010), a PC for data retrieval, a furnace and various cold traps. Before each run, the samples were

oxidized in a 50 mL min^{-1} flow of 20 vol.% O_2 in He at 300 °C for 30 min. After that, helium was admitted to remove oxygen and finally, the system was cooled to 25 °C. The samples were subsequently contacted with a 50 mL min^{-1} flow of 5 vol. % H_2 in N_2, heated at a rate of 5 °C min^{-1}, from 25 °C to a final temperature of 700 °C and held at 700 °C for 1 h. Hydrogen consumption was monitored by a thermal conductivity detector after removing the formed water. The characteristic number P proposed by Malet and Caballero [21] defined as $\beta S_o/V^*C_o$, where S_o is the initial amount of reducible species in the sample (μmol), V* is the total flow rate (mL min^{-1}), C_o the initial hydrogen concentration in the feed (μmol min^{-1}) and β the heating rate (°C min^{-1}) was ≈ 10 °C in order to obtain an unperturbed reduction profile.

Raman spectroscopy. The Raman spectra were recorded using a Lab Ram spectrometer (Jobin-Yvon) coupled to an Olympus confocal microscope (100X objective lens was used for simultaneous illumination and collection), equipped with a CCD with the detector cooled to about -70 °C using the Peltier effect. The excitation wavelength was in all cases 532 nm (Spectra Physics argon-ion laser). The laser power was set at 30 mW. Integration times ranged from a few seconds to a few minutes depending on the sample. A scanning range between 100 and 2000 cm^{-1} was applied.

Scanning electron microscopy and energy dispersive X-ray spectroscopy (SEM-EDX). Scanning electron micrographs were obtained in a LEO 1450 VP. This instrument, equipped with an energy dispersive X-ray microanalyzer (EDAX Genesis 2000) and a Si(Li) detector, allowed the analytical electron microscopy measurements. The samples were sputter coated with gold.

2.3. Catalytic test

The ethanol steam reforming reaction was carried out in a fixed-bed quartz tubular reactor operated at atmospheric pressure. The reactor is encased in a furnace which is controlled by a programmable temperature controller. The reaction temperature was measured with a coaxial thermocouple. The feed was a gas mixture of ethanol, water and helium (free of oxygen). Ethanol and water were fed through independent saturators before mixing. The flow rates of gas stream were controlled by mass flowmeters. The flow rate was 70 mL min^{-1} at room temperature with an ethanol molar composition of 3%. The H_2O:C_2H_5OH molar ratio was 3.6-3.8 in all the experiments. The catalyst weight was 300 mg (0.3-0.4 mm particle size range selected after preliminary mass transport experiments to minimize diffusional resistances). The catalyst, without a previous reduction, was heated to the reaction

temperature under He flow, then the mixture with C_2H_5OH + H_2O was allowed to enter into the reactor to carry out the catalytic test. In all the cases fresh samples were used. The reactants and reaction products were analyzed on-line by gas chromatography. H_2, CH_4, CO_2 and H_2O were separated by a 1.8 m Carbosphere (80-100 mesh) column and analyzed by TC detector. Besides, CO was analyzed by a flame ionization detector after passing through a methanizer. Higher hydrocarbons and oxygenated products (C_2H_4O, C_2H_4, C_3H_6O, C_2H_5OH, etc.) were separated in RT-UPLOT capillary column and analyzed with FID using N_2 as a carrier gas. The activity was measured at 500 and 600 °C, for four hours at each temperature.

3.- Results and discussion

3.1. *Structural features*

Some characteristics of CoZnAl catalysts with 9 and 25 wt.% Co are compiled in Table 1. The Zn/Al molar ratio was kept nearly constant and slightly greater than 0.5 which is the stoichiometric value to form $ZnAl_2O_4$. In both cases, homogeneous precursors were obtained and their decompositions were studied by thermogravimetry. The TG curves for 9 and 25 wt.% Co (not shown) obtained under a N_2 flow presented an important weight loss (68.8 and 68.3% of the original weight, respectively) centered at 411 and 416 °C, respectively. Taking into account these results, the first step of the calcination procedure was carried out at 450 °C under nitrogen flow as it was described in the experimental part.

Specific surface areas shown in Table 1 are similar and low compatible with the relatively high calcination temperature. The calcination temperature was chosen to ensure that there will be no structural changes in the catalyst within the temperature range used for ethanol steam reforming.

The X-ray patterns of catalysts CoZA9 and CoZA25 fresh are shown in Figs. 1 (a) and 2 (a). In both samples, diffraction lines at 2θ = 36.9°, 31.3°, 44.8°, 55.6°, 59.4° and 65.3° are observed. They are assigned to a highly crystalline $ZnAl_2O_4$ spinel (JCPDS-5-669) and also to the presence of Co_3O_4 (JCPDS-42-1467) and/or $CoAl_2O_4$ (JCPDS-10-0458) which reflection lines are coincident. Lines corresponding to CoO (2θ = 34.1°, 39.6º, 57.3º and 68.4°, JCPDS-42-1300; 2θ = 42.4°, 36.5º, 61.5º and 73.7º, JCPDS-43-1004) are not detected. If this phase is present it is in an amorphous way or with a particle size lower than the technique detection limit. Besides, on the sample with Co loading 9 wt.% weak bands corresponding to ZnO (2θ = 36.2°, 31.8°, 34.4°, JCPDS-36-1451) are also observed. The presence of ZnO could indicate

that a fraction of aluminum is combined with the cobalt likely forming $CoAl_2O_4$ on CoZA9. In literature, it has been reported that Co is present as Co_3O_4 on Co/Al_2O_3 (15 wt. % Co) when the catalyst prepared by wet impregnation method was calcined in air at 600 ºC, whereas the spinel phase $CoAl_2O_4$ and CoO appeared after being used in the reaction with a previous reduction [17]. However, in ternary system Cu-Co-Al prepared by coprecipitation was reported that the samples calcined in air exhibited the formation of Co_3O_4 and $CoAl_2O_4$ spinels [22].

The reducibility of CoZnAl catalysts is examined by temperature programmed reduction, Fig. 3. The TPR for the catalyst with 9 wt.% Co, profile (a), shows a main peak of hydrogen consumption at 700 ºC ascribed to the reduction of Co^{+2} species which are strongly interacting with $ZnAl_2O_4$ or forming $CoAl_2O_4$. Besides, the shoulder at 597 ºC suggests the presence of Co species in different extent of interaction with the aluminate phase. A similar behavior was reported in literature by Batista et al. [23] on Co/Al_2O_3 catalysts with 8 and 18 wt.% Co. The TPR for catalyst with 25 wt.% Co, profile (b), clearly shows two peaks of hydrogen consumption. The peak at low temperature, centered at 444 ºC, could be attributed to the reduction of Co^{+2}/Co^{+3} (Co_3O_4). De la Peña O'Shea et al.[24] carried out a study of the evolution of Co_3O_4 during hydrogen reduction under *operando* conditions by XRD measurements. The XRD patterns obtained *in situ* during the H_2 treatment showed that peaks, due to reflections of Co_3O_4, disappeared when the temperature increased to 325 °C. At this temperature, the presence of CoO could be deduced from XRD pattern. When the temperature was 350 °C, CoO started to transform into fcc Co. Taking into account this information, it could be inferred that the presence of zinc aluminate phase decreases the reducibility of Co^{+2}/Co^{+3}. The second hydrogen consumption band, between 635-700 ºC, could again be assigned to the reduction of strongly interacted Co^{+2} with the spinel phase $ZnAl_2O_4$ or forming a $CoAl_2O_4$ phase. When pure $CoAl_2O_4$ prepared by the citrate method was reduced under the same TPR conditions only one peak at 679 °C was observed. On $Co/\gamma\text{-}Al_2O_3$ catalysts, strong interactions between Co species and the support have been reported in literature [25]. Besides, the Al^{3+} ions polarize the Co-O bond which is lightly covalent increasing the effective charge of Co and the reticular energy [26]. Thus, $CoAl_2O_4$ requires a higher temperature to be reduced and it would only be partially reduced under the reforming conditions used in this work.

The X-ray patterns of reduced samples showed in Figs. 1 (b) and 2 (b) reveal that $ZnAl_2O_4$ is not reduced under these conditions [27]. Wide peaks of low intensity

corresponding to Co^0 (2θ = 44.3°, 51.4°, 75.8°, JCPDS-15-0806) are also detected. This could indicate that the Co^0 particles are small and they would be dispersed into the aluminate matrix. It is also important to take into account that XRD patterns were *ex-situ* registered and as cobalt is a pyrophoric material, the reoxidation could occur.

With the aim of elucidating that Co species are being reduced under TPR conditions (Co_3O_4 o $CoAl_2O_4$), the hydrogen consumption was estimated by the integration of the H_2-TPR peaks and it is shown in Table 2. The theoretical H_2/Co molar ratio for Co_3O_4 ($Co_3O_4 + 4\,H_2 \rightarrow 3\,Co^0 + H_2O$) is 1.33 and for $CoAl_2O_4$ ($CoAl_2O_4 + H_2 \rightarrow Co^0 + Al_2O_3 + H_2O$) is 1. Then, within the experimental errors, it can be determined that Co^{2+} species are mainly present in the catalyst with low Co loading (9%) whereas both species Co^{2+}/Co^{3+} should be present in the sample with a high Co loading (25%).

RAMAN spectra for CoZA9 and CoZA25 catalysts are shown in Fig.4. Broad Raman bands between 400 and 750 cm^{-1} are observed for both samples in different conditions: fresh, reduced under TPR conditions and after being used in the reforming reaction. Raman bands corresponding to pure Co compounds are shown in Table 3 [25, 28]. The main peaks of $ZnAl_2O_4$ occur at ~660 and ~425 cm^{-1} [29]. The Raman bands of fresh catalysts are clearly not identical to those of $CoAl_2O_4$ or Co_3O_4. Jongsomjit et al. [28] have reported similar results on Co/Al_2O_3 catalysts and these authors have suggested that these broad Raman bands represent a surface nonstoichiometric Co spinel (Co_xO_y-Al_2O_3). The phase where Co ions occupy tetrahedral positions in the Al_2O_3 lattice is usually assumed to be $CoAl_2O_4$. Besides, it is well known the very high tendency of Co to occupy octahedral sites as such Co_3O_4 and $Co(Co,Al)_2O_4$ inverse spinel [30, 31]. On CoZnAl catalysts this Co "aluminate" could be formed as a consequence to the strong interaction of Co species with $ZnAl_2O_4$ in agreement with TPR results. The Raman spectra of both reduced samples show a similar appearance with a significant decrease in the band intensities, indicating the reduction of Co species.

3.2. Catalytic steam reforming results

The activity of CoZA9 and CoZA25 catalysts is tested in ethanol steam reforming at 500 and 600 °C. The product distributions as a function of time are shown in Figs. 5 and 6. Although pure $ZnAl_2O_4$ spinel has shown to be active [32], the introduction of cobalt produces a catalyst with a much better performance for hydrogen production.

At 500 ºC, both samples are equally active with ethanol conversions of 100%. At this temperature, apart from CO_2, CO, CH_4 and H_2, other products such as C_2H_4, C_3H_6, CH_3COCH_3 and CH_3CHO are obtained. In Table 4, the selectivities to each product at 70 min in time on stream are compared. The main products for catalyst with 9 wt.% Co are CH_3CHO, CH_3COCH_3, CO_2 and CH_4. A minor amount of C_3 (propane-propilene), C_2H_4 and small amounts of CO are also detected in agreement with literature data on Co based catalysts [15]. After 2 h in reaction the selectivity to CH_3COCH_3 increases from 24 to 39%, while the opposite occurs for acetaldehyde (from 31.7 to 24.6%) and hydrogen (from 2.1 to 1.9 mol H_2/mol C_2H_5OH). The other products remain almost constant. For CoZA25, the main products are CO_2, CH_3CHO, CH_4 and CH_3COCH_3. The acetone selectivity increases from 17.2 to 22.8% while selectivities to CO_2, CH_3CHO and CH_4 slightly decrease. The hydrogen yield is almost constant (2.5- 2.6 mol H_2/mol C_2H_5OH). The H_2 selectivity (assuming that a selectivity of 100% corresponds to 6 mol H_2/mol C_2H_5OH) increases from 36.7% to 43.3% with increasing Co loading. Small amounts of C_2H_4, C_3 and CO are also observed. Similar results were found on Co(18%)/Al_2O_3 at 400 °C by Batista et al. [23]. These authors have reported that the CO formation decreases with the increase the Co loading. Over CoZnAl catalysts a slight decrease in CO selectivity is observed at 500 °C but this tendency is opposite when the reaction temperature increases. It is important to note that these catalysts are partially reduced under the reforming conditions.

The differences in the catalytic behavior are more important at 600 °C. For the sample with 9 wt.% Co, the selectivity to acetaldehyde increases from 6.6 to 50% after 200 min in time on stream while CO_2, CH_4 and H_2 decrease. Simultaneously, the ethanol conversion decreases from 100% to 71.8%, Fig. 6(a). This behavior could be related to dehydrogenation reaction from ethanol ($C_2H_5OH \rightarrow C_2H_4O + H_2$) and reforming of acetaldehyde ($C_2H_4O + H_2O \rightarrow CH_4 + CO_2 + 2H_2$). The H_2 yield is 1.1 mol H_2/mol C_2H_5OH after this time.

At 600 °C the ethanol conversion on the CoZA25 remains complete and the only reaction products are H_2, CO, CO_2 and CH_4. A transient step of 100 min is observed where changes in product distribution are detected. This could be attributed to the simultaneous occurrence of a deeper reduction process and the reforming reactions. During this period the H_2 detected is lower which could be an indication of its consumption due to the major degree of reduction of this sample. The hydrogen yield is 4.7 mol H_2 /mol C_2H_5OH after one hour in time on stream, Table 3, which represents a selectivity of 78%. In steady state the selectivity

to CO is high being the CO/CO_2 molar ratio ≈ 1.9 and the H_2 selectivity reaches 86%. The main reactions involved are $C_2H_5OH + H_2O \rightarrow CH_4 + CO_2 + 2H_2$ and $CH_4 + 2H_2O \rightarrow CO_2 + 4H_2$, with a WGS reverse contribution ($CO + H_2O \leftrightarrow CO_2 + H_2$). Similar results have been reported in literature when Co catalysts are tested in steam reforming of ethanol at temperatures higher than 400 °C [1, 8, 11, 16]. Besides, it is also reported C_2H_4 formation and an important amount of carbon deposits, particularly, when alumina is used as support. On CoZnAl catalysts, the carbon deposition (further shown) and C_2H_4 formation are low. In fact C_2H_4 is not observed on CoZA25 at 600 °C. These differences could be attributed to differences in experimental conditions and in the spinel properties.

The improved catalytic behavior on CoZA25 could be related to a greater fraction of Co^{n+} (n = 2 or 3) reduced under reforming conditions which remains in the $ZnAl_2O_4$ matrix either as Co^0 or mostly as Co species in low oxidation states.

3.3 Characterization post reaction of catalysts

The diffraction patterns of CoZnAl catalysts used in reaction at 500 and 600°C are shown in Figs. 1 (c-d) and 2 (c-d). In all the cases, they reveal the reflexion lines corresponding to $ZnAl_2O_4$ and $CoAl_2O_4/Co_3O_4$. For CoZA9, non significant changes are detected in fresh and used samples by XRD. The diffraction peaks of reduced cobalt species are not seen, probably they are present in only very thin surface layers and consequently, they are XRD invisible. For CoZA25, weak peaks assigned to Co^0 are also observed. These results indicate that this catalyst has suffered a higher reduction extent under reforming conditions and the Co particles are in small size. In comparison with XRD patterns of fresh and H_2 reduced samples, the most important difference is in the 2θ = 40º to 45º range where a peak overlap is clearly observed. One of them could be attributed to the (200) plane of CoO at 2θ = 42.4º (JCPDS-43-1004). It could be inferred that only a fraction of Co species is reduced to CoO and Co^0 under reforming conditions. These results are in agreement with others from literature [17]. The Raman spectra of used catalysts are also shown in Fig.4. The spectra recorded represent the sum of the Raman bands of $ZnAl_2O_4$, CoO, Co_3O_4 and $CoAl_2O_4$, and no significant differences are observed.

In Fig. 7, TG curves of used CoZnAl catalysts at 500 and 600 °C reaction temperatures are shown. For CoZA9 and CoZA25 at 500 ºC, a small weight loss (1.1- 1.4%)

is observed from room temperature to 400 ºC (curves a and c). The water desorption and/or adsorbed species from atmosphere (until 120 °C) and the carbon combustion (until 400 °C) could be responsible of these losses. For samples used in reaction at 600 ºC (curves b and d), the behavior is different. For CoZA9 sample, an abrupt weight loss (2.1 wt.%) centered at 362°C is observed which could be attributed to carbon combustion. This carbon could be deposited on metallic Co species and/or on the aluminate matrix. For CoZA25 sample, the TG curve shows different steps: the first zone corresponds to water desorption (room temperature to 120 ºC), followed by a constant weight until 220 ºC. Then, it is observed a weight increase until 450 °C probably due to Co oxidation. Finally, there is a weight loss (1.05 wt.%) between 450 and 550 °C which could be related to simultaneous processes of Co oxidation and carbon deposit combustion. Cavallaro et al. [33] have reported deactivation on Co/Al_2O_3 catalysts (20 wt.% Co) under reforming conditions at 650 ºC as a consequence of Co oxidation and coque formation but the amount of C was not quantified. Batista et al. [16] have also detected coque formation over Co based catalysts (8-18 wt.% Co) at 400 °C and 9 h of steam reforming. The amount of coke was markedly higher (24.6 wt.% on Co/Al_2O_3 > 17 wt.% on Co/MgO > 14.2 wt.% on Co/SiO_2) though the experimental conditions are not totally comparable. It is well established that the more ordered the carbon structure, the higher is the temperature required for gasification during TPO [34, 35]. The carbon deposit is oxidized at a relatively low temperature on CoZA9 catalyst what suggests a low degree of graphitization. This is in agreement with XRD analyses (figures 1) where the typical peak at *ca* 26° corresponding to graphitic carbon is not detected. Since the oxidation temperature in TPO analysis is around 500 °C on CoZA25 used at 600 °C, a slightly enhanced structural order in carbon deposit could be indirectly inferred. However, the typical Raman bands centered at 1593 cm^{-1} and 1350 cm^{-1} assigned to ordered carbon, graphitic type, and disordered defective structures, respectively [36], are not clearly observed on used samples (spectra not shown).

The presence of carbon deposits over the catalysts used in reaction is also examined by SEM. The micrographs for catalysts tested at 600 ºC, Figs. 8 A) CoZA9 and B) CoZA25, reveal particles with different morphology: plane particles and others with rugous appearance. When the carbon quantification is done on two different zones: a) and b), differences in the carbon quantity are observed. For the sample CoZA9 tested at 600 °C, in zone a) the value of carbon obtained is 4.6%, and in zone b) it is of 9.7%. On the other hand, for the CoZA25 sample, the quantitative analysis allowed us to find a quantity of carbon larger than in the rest of the analyzed samples. Thus, the EDX results showed 21% of carbon in zone a) and 41% in

zone b). With these results it can be inferred that carbon deposition is not homogeneous (which could explain the Raman results) but that it is principally deposited in the rugous particles. Consequently, it can be said that larger the quantity of Co, more deposited carbon. Similar results were observed on samples tested at 500 °C (not shown). Within the detection limit of the technique, carbon filaments are not observed and the presence of amorphous carbon could be inferred.

4. Conclusions

The catalytic behavior of CoZnAl catalysts in the ethanol steam reforming reaction under high conversion values and low C_2H_5OH:H_2O (3.6-3.8) molar ratio was studied. The catalysts were prepared by the citrate method and the amounts of cobalt were 9 and 25 wt%. The preparation method led to the formation of spinel matrix mainly $ZnAl_2O_4$. A nonstoichiometric $CoAl_2O_4$ was mainly formed on CoZA9 whereas this "aluminate" and Co_3O_4 were detected on CoZA25.

The catalysts without a previous reduction were very active in the steam reforming of ethanol, with 100% of ethanol conversion at 500 and 600 °C. The increase in Co loading decreased the formation of intermediate compounds and improved the H_2 selectivity. At 600 °C, the hydrogen selectivity increases from 31% to 86% when Co loading increases from 9 to 25%. This improved behavior was related to the presence of Co_3O_4 on CoZA25 which was mostly reduced to Co^0 and CoO under reforming conditions.

The CoZA25 working at 600 °C showed good stability after 300 min in operation. CO, CO_2 and minor amounts of CH_4 were the only carbon products and the hydrogen production was very high (86%). Small amounts of carbon not homogeneously distributed on catalyst surface were detected but they did not affect conversion and selectivity under the operation conditions used in this work.

Acknowledgments

Financial supports are acknowledged to CONICET, ANPCyT and Universidad Nacional de San Luis. The authors wish to thank Dr. John Múnera for Raman assistance. The funds from the ANPCyT to buy the Raman instrument are also grateful (PME 87-PAE 36985).

References

[1] P. Ramírez de la Piscina, N. Homs, Chem. Soc. Rev. 37 (2008) 2459.

[2] R. M. Navarro, M.A. Peña, J. L.G. Fierro. Chem. Rev. 107 (2007) 3952

[3] A.N. Fatsikostas, D.I. Kondarides, X.E. Verykios, Catal. Today 75 (2002) 145.

[4] S. Freni, S. Cavallaro, N. Mondello, L. Spadaro, F. Frusteri, Catal. Commun. 4 (2003) 259.

[5] M. N. Barroso, M. F. Gomez, L. A. Arrúa, M. C. Abello. Appl. Catal. A 304 (2006) 116.

[6] F. Mariño, G. Baronetti, M. Jobbagy, M. Laborde, Appl. Catal. A 238 (2003) 41.

[7] V. Klouz, V. Fierro, P. Denton, H. Katz, J.P. Lisse, S. Bouvot-Mauduit, C. Mirodatos, J. Power Sources 105 (2002) 26.

[8] J.P. Breen, R. Burch, H.M. Coleman, Appl. Catal. B 39 (2002) 65.

[9] V.V. Galvita, G.L. Semin, V.D. Belyaev, V.A. Semikolenov, P. Tsiakaras, V.A. Sobyanin, Appl. Catal. A 220 (2001) 123.

[10] F. Auprêtre, C. Descorme, D. Duprez, Catal. Commun. 3 (2002) 267.

[11] D.K. Liguras, I. Kondarides, X.E. Verykios, Appl. Catal. B 43 (2003) 345.

[12] F. Haga, T. Nakajima, H. Miya, S. Mishima, Catal. Lett. 48 (1997) 223.

[13] J. Llorca, N. Homs, J. Sales, P. Ramírez de la Piscina, J. Catal. 209 (2002) 306.

[14] J. Llorca, J.A. Dalmon, P. Ramírez de la Piscina, N. Homs, Appl. Catal. A 243 (2003) 261.

[15] J. Llorca, P. Ramírez de la Piscina, J.A. Dalmon, J. Sales, N. Homs, Appl. Catal. B 43 (2003) 355.

[16] M.C. Batista, R.K.S. Santos, E.M. Assaf, J.M. Assaf, E.A. Ticianelli, J. Power Sources 124 (2003) 99.

[17] D.R. Sahoo, Shilpi Vajpai, Sanjay Patel, K.K. Pant. Chem. Eng. J. 125 (2007) 139.

[18] H. Song, L. Z. Zhang, U.Ozkan, Catal. Today 129 (2007) 346.

[19] S. S-Y Lin, D. H. Kim, S.Y. Ha, Appl. Catal A: 355 (2009) 69.

[20] H. Song, U. Ozkan, J. Catal. 261 (2009) 66.

[21] P. Malet, A. Caballero, J. Chem. Soc. Faraday Trans. 84 (1988) 2369.

[22] A. J. Marchi, J. I. Di Cosimo, C. R. Apesteguía, Catal. Today 15 (1992) 383.

[23] M.C. Batista, R.K.S. Santos, E.M. Assaf, J.M. Assaf, E.A. Ticianelli, J. Power Sources 134 (2004) 27.

[24] V.A. de la Peña O'Shea, N. Homs, E. B. Pereira, R. Nafria, P. Ramirez de la Piscina, Catal. Today 126 (2007) 148.

[25] B. Jongsomjit, J. G. Goodwin Jr. Catal. Today 77 (2002) 191.

[26] P. Arnouldy, J.A. Moulijn, J. Catal. 93 (1985) 18.

[27] M. Barroso, M. Gomez, J.A. Gamboa, L. Arrua, M. C. Abello, J. Phys. Chem. Sol. 67 (2006) 1583.

[28] B. Jongsomjit, J. Panpranot, J. G. Goodwin Jr., J. Catal. 204 (2001) 98.

[29] C. M. Fang, C-K Long., G.A. de Wijs, G. de With, Physical Rev. B. 66 (2002) 144301.

[30] T. Baird, K. Campbell, P. Holliman, P. Hoyle, D. Stirling, B. Williams, M. Morris, J. Mater. Chem. 7 (1997) 319.

[31] P. Benito, M. Herrero, F. Babajos, V. Rives, C. Royo, N. Latorre, A. Monzón, Chem. Eng. J. 149 (2009) 455.

[32] M. Barroso, M. Gomez, L. Arrua, M. C. Abello, Catal. Lett. 109 (2006) 13.

[33] S. Cavallaro, N. Mondello, S. Freni. J. Power Sources 102 (2001) 198.

[34] S. Natesakhawat, R. Watson, X. Wang, U. Ozkan, J. Catal. 234 (2005) 496.

[35] M. C. Sanchez-Sanchez, R. M. Navarro, J.L.G. Fierro, Int. J. Hydrogen Energy 32 (2007) 1462.

[36] F. Pompeo, N. Nichio, O. Ferretti, D. Resasco, Int. J. Hydrogen Energy 30 (2005) 1399.

Figure captions

Figure 1. Diffraction patterns of CoZA9 catalysts; (a) fresh; (b) reduced; (c) after being used at 500 °C; (d) after being used at 600 °C. ❖: $ZnAl_2O_4$, ■: ZnO, ◊ :$CoAl_2O_4$ and/or Co_3O_4, ⓿: Co^o.

Figure 2. Diffraction patterns of fresh CoZA25 catalysts (a) fresh; (b) reduced; (c) after being used at 500 °C; (d) after being used at 600 °C. ❖: $ZnAl_2O_4$, ■:ZnO, ◊:$CoAl_2O_4$ and/or Co_3O_4, ⓿: Co^o.

Figure 3. TPR profiles of CoZnAl catalysts. (a) CoZA9; (b) CoZA25.

Figure 4. Raman spectra of (a) CoZA9 and (b) CoZA25 catalysts

Figure 5. Product distribution in the ethanol steam reforming at 500 ºC on (a) CoZA9 and (b) CoZA25 catalysts. ❍: H_2, ★: CH_4, ●: CO_2, ▼: CO, ■: C_2H_4O, ▲: C_3H_6O, ◆: C_2H_4 and □: C_3H_6. Ethanol conversion: 100%

Figure 6. Product distribution in the ethanol steam reforming at 600 ºC on (a) CoZA9 and (b) CoZA25 catalysts. ❍: H_2, ★: CH_4, ●: CO_2, ▼: CO, ■: C_2H_4O, ▲: C_3H_6O, ◆: C_2H_4 and □: C_3H_6. In figure (6a), ⊗ represents ethanol conversion and in figure (6b), ethanol conversion 100%.

Figure 7. TG curves of thermal decomposition of used catalysts: CoZA9 at reaction temperature (a) 500 °C and (b) 600 °C: CoZA25 at reaction temperature (c) 500 °C and (d) 600 °C.

Figure 8. SEM micrographs and EDX spectra of catalysts after ethanol steam reforming at 600 °C. A) CoZA9 (10.57 kx) and B) CoZA25 (6.17 kx).

Table 1. Characteristics of CoZnAl catalysts prepared by citrate method

Catalyst	Co wt.%	Zn wt.%	Al wt.%	Zn/Al	S_{BET}, m^2 g^{-1}
CoZA9	9.3	31.1	20.3	0.63	20.4
CoZA25	24.7	31.4	20.5	0.63	19.3

Table 2. Reduction temperature and H_2/Co molar ratio in TPR experiments

Catalyst	Temperature (ºC)		H_2/Co
	1st peak	2nd peak	(mol/mol)
CoZA9	596	700	1.02
CoZA25	444	634	1.13

Table 3. Raman bands of pure compounds [25, 28]

Raman Shift, cm^{-1}	198	412	480	519	619	690	753
$CoAl_2O_4$	s	w	m	s	s	s	m
Co_3O_4	s	--	m	w	w	s	--
CoO	m	--	m	w	w	s	--

s: strong; m: medium; w: weak

Table 4. Catalytic results in ethanol steam reforming at 500 and 600 °C on CoZnAl catalysts

	T, °C	**Time min**	**Y_{CH4} %**	**Y_{CO} %**	**Y_{CO2} %**	**Y_{CH} %**	**Mol H_2/ mol C_2H_5OH**
CoZA9	500	69	12.6	2.2	18.7	66.5	2.2
	600	58	34.8	5.4	38.2	21.7	2.5
CoZA25	500	74	19.8	1.9	33.5	44.8	2.6
	600	64	7.6	54	38.4	0	4.7

Ethanol conversion: 100%; Y: yield; T: reaction temperature; CH = C_2H_4+ C_3H_6+ CH_3COCH_3+ CH_3CHO

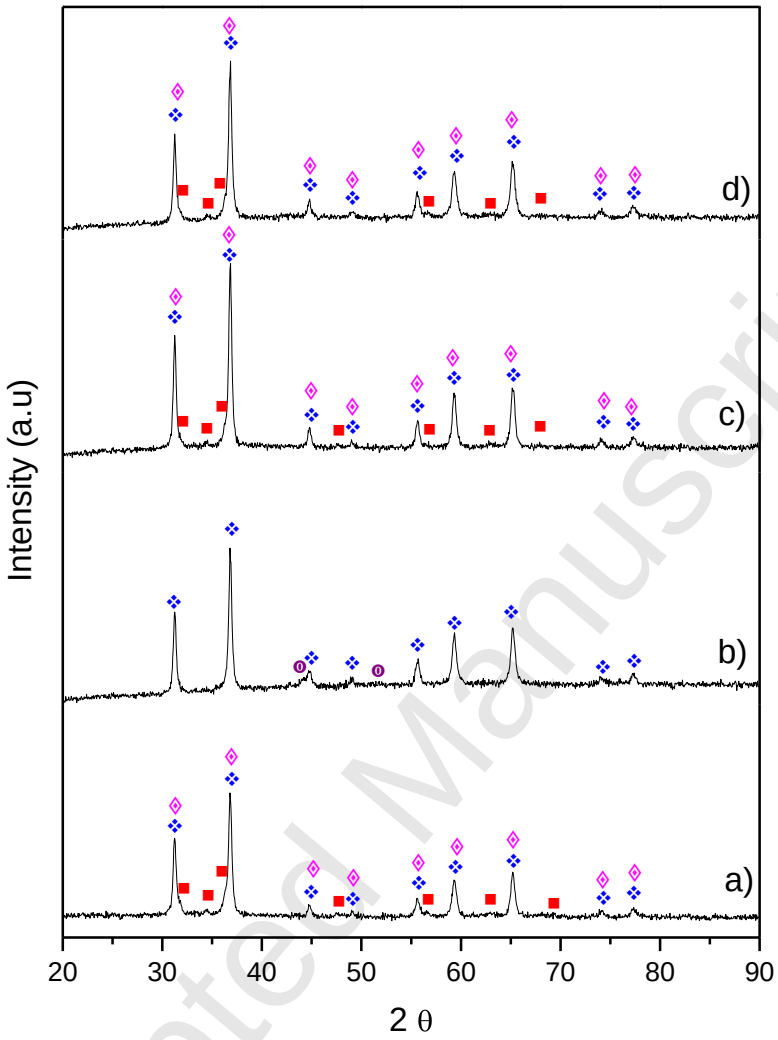

Figure 1

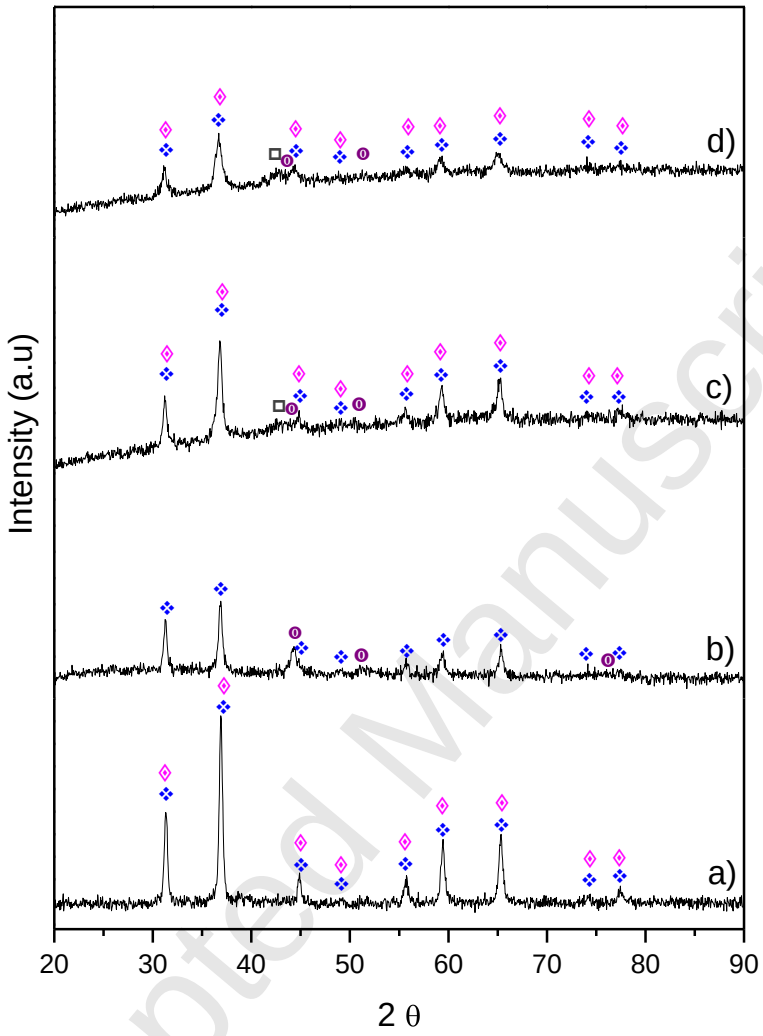

Figure 2

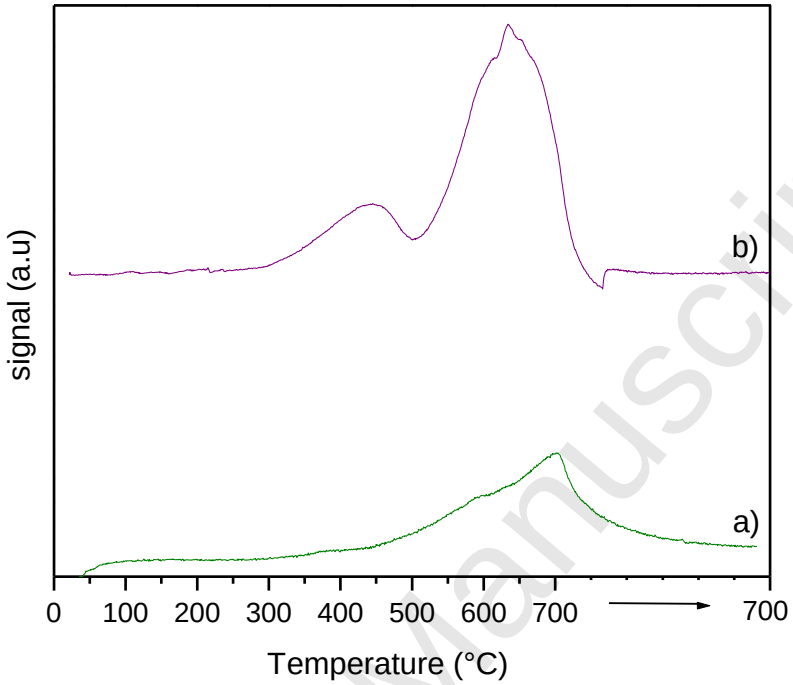

Figure 3

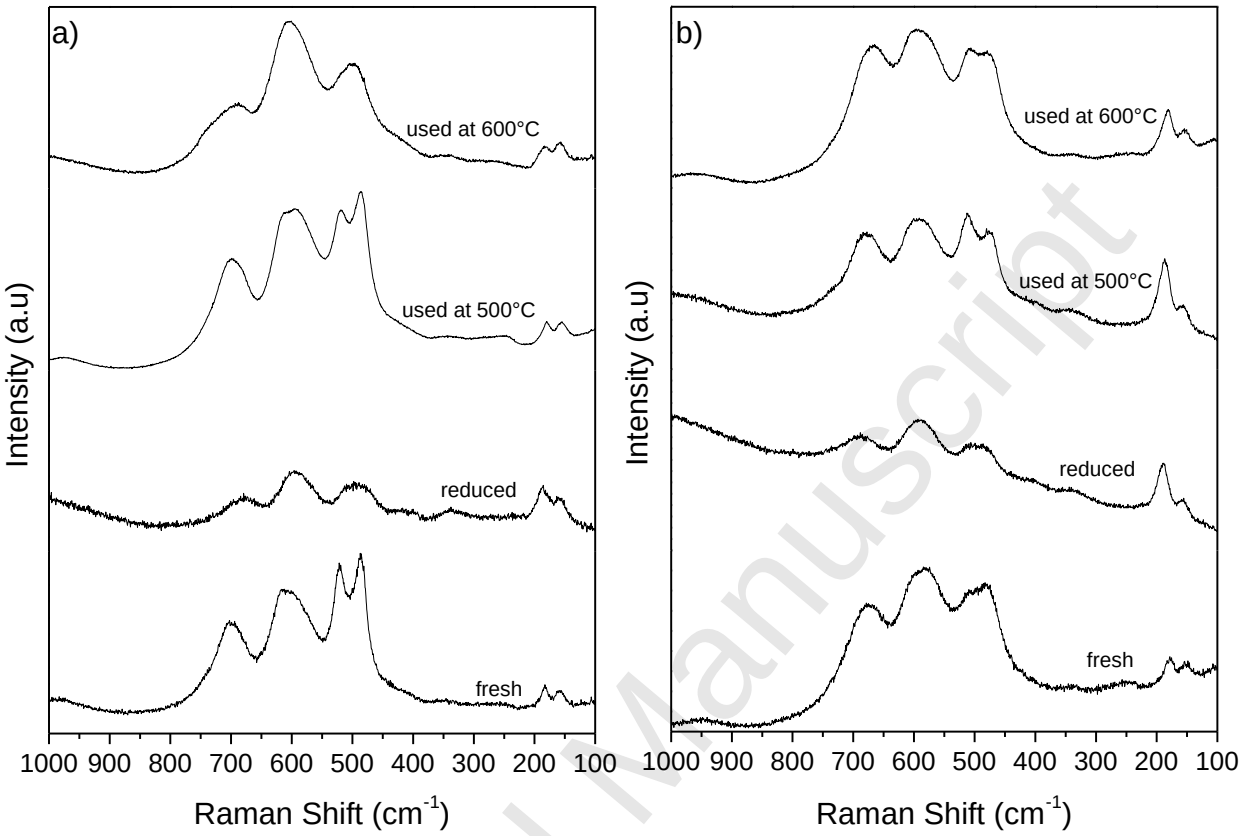

Figure 4

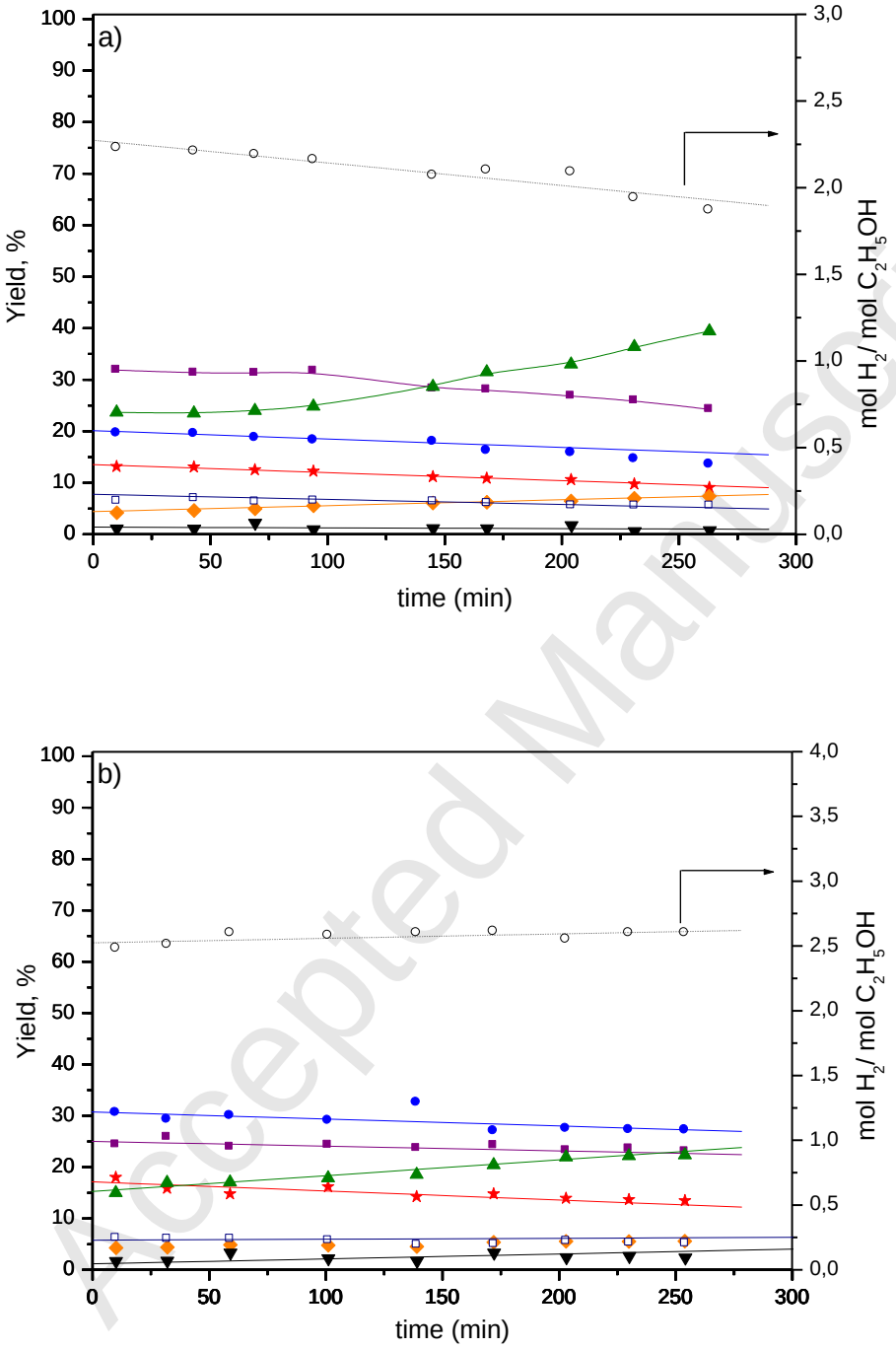

Figure 5

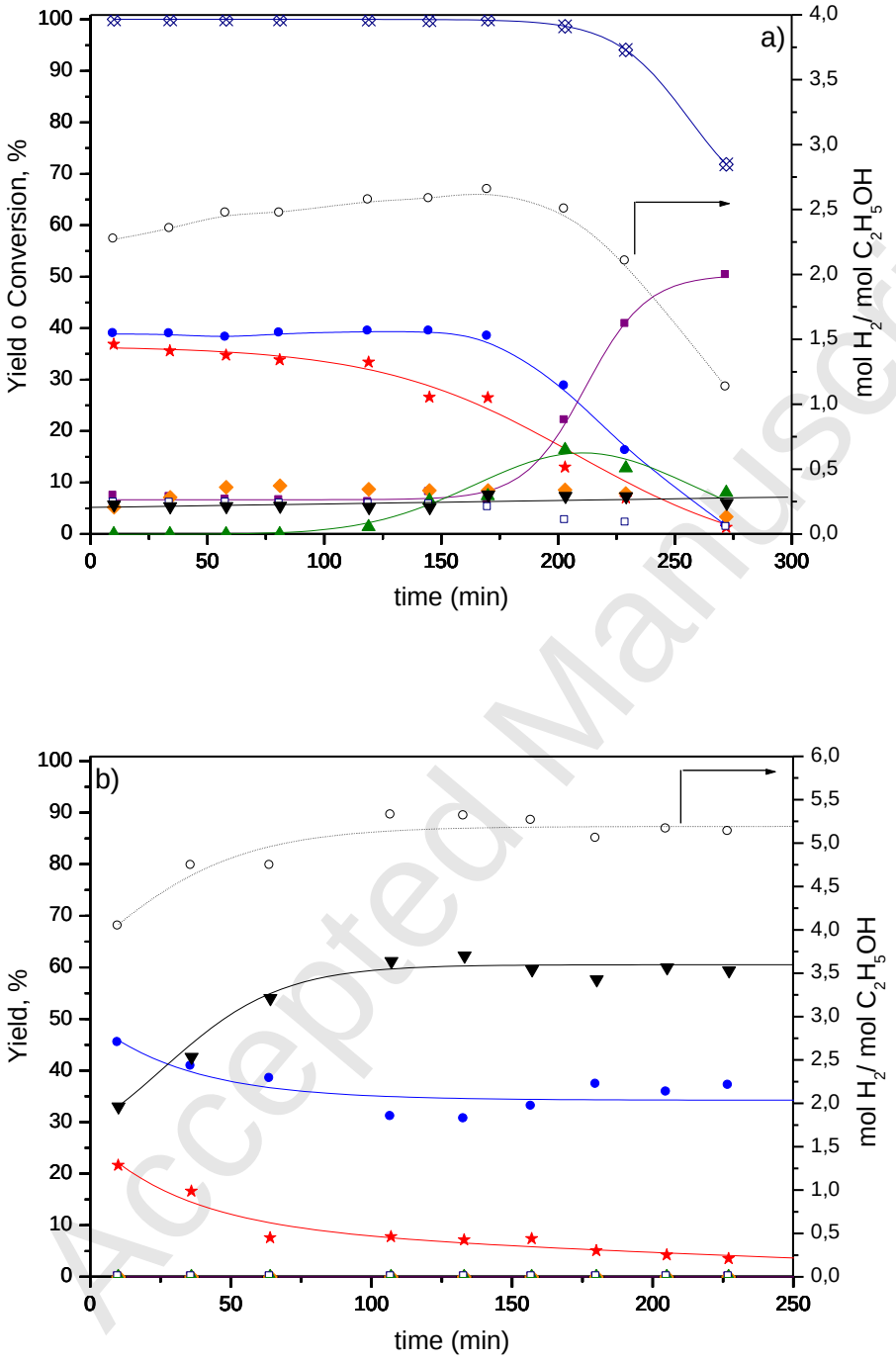

Figure 6

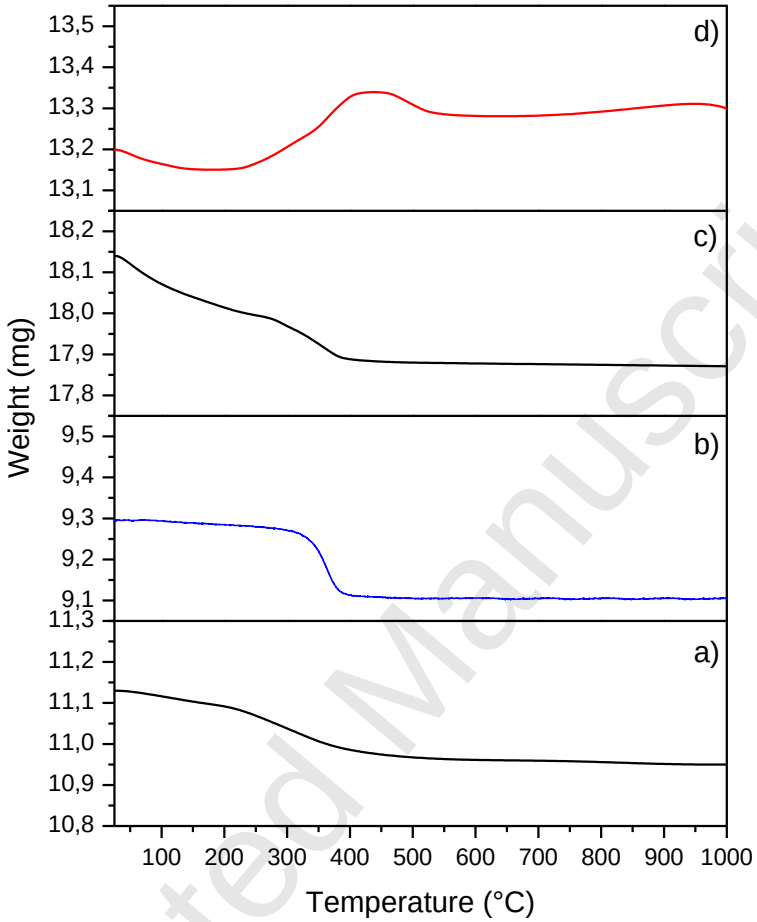

Figure 7

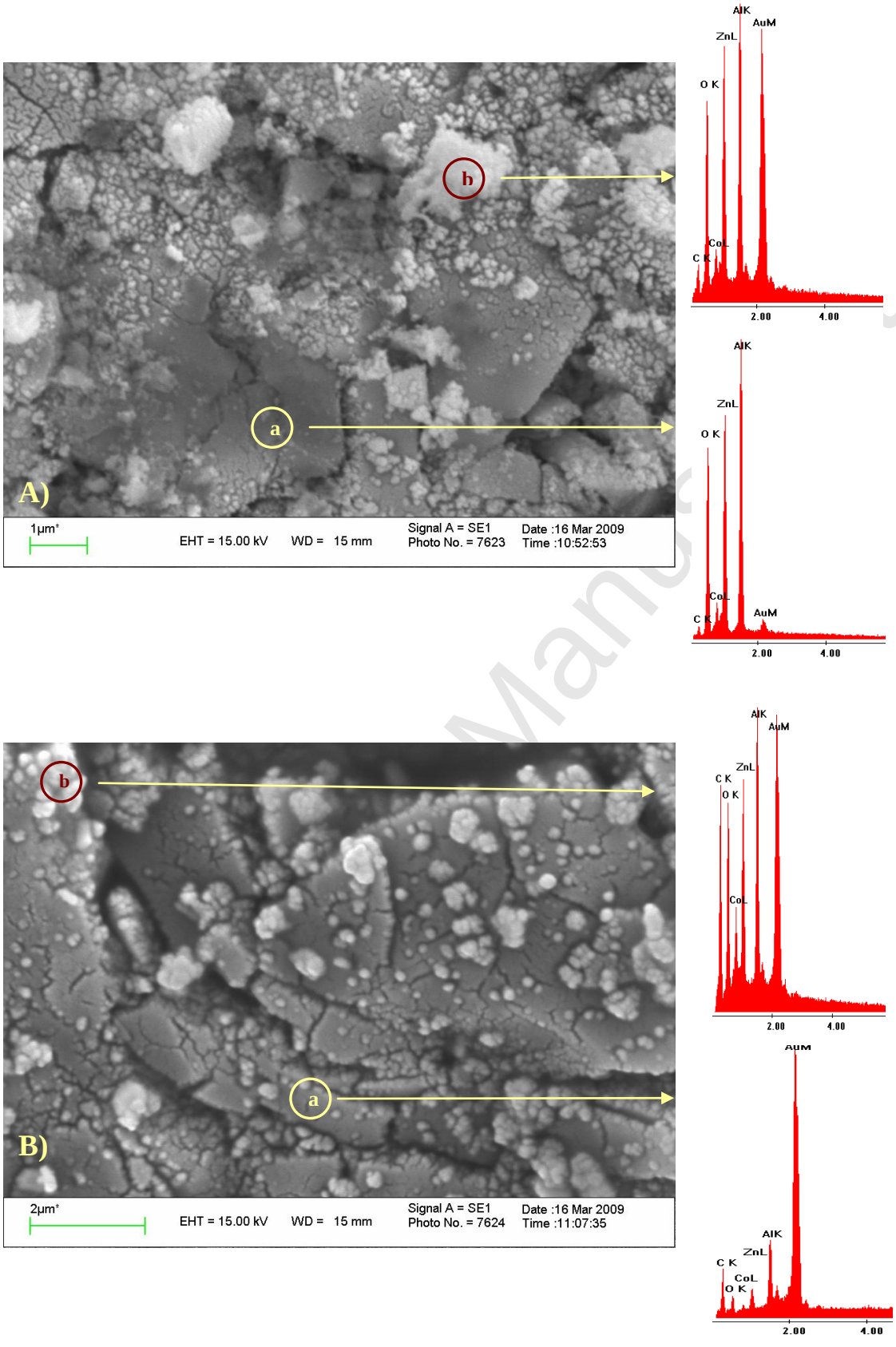

Figure 8